

A 23-Year Nationwide Study Revealing Aerosol-Driven Light Rain Shifts in China's Emission Control Era

Rou Zhang¹, Xiaoxiao Huang¹, Pu Wang¹, Guiquan Liu¹, Mengyu Liu¹, Songjian Zou¹, Lu Chen², Fang Zhang^{1*}

¹School of Ecology and Environment, College of Artificial Intelligence, Harbin Institute of Technology (Shenzhen), Shenzhen 518055, China

²School of Urban and Planning, Yancheng Teachers University, Yancheng, 224051, China

Correspondence to: Fang Zhang (zhangfang2021@hit.edu.cn)

Abstract. Precipitation dynamics critically regulate Earth's hydrological cycle and climate system, yet the mechanisms driving decadal-scale variations in light rain remain poorly quantified. Our analysis of a 23-year (2000–2022) national-scale dataset reveals contrasting trends in light precipitation occurrence: a significant decline (1.0 days yr⁻¹, p < 0.05) during 2000–2013 followed by a pronounced increase (1.9 days yr⁻¹, p < 0.01) in 2013–2022. Cross-temporal analysis demonstrates a national wide inverse correlation (r = -0.55, p < 0.01) between aerosol concentrations and light rain frequency in the China's Emission Control Era, when the PM_{2.5} shows an upward trajectory before 2013 followed by a markedly downward decline thereafter, providing a natural experiment to quantify aerosol effects in precipitation. Through multi-algorithm machine learning and causal inference modeling, we further identify aerosol-cloud microphysical processes as the dominant driver, with PM_{2.5} concentration changes explaining 59-63% of the decadal trends of light rain. As a result, the PM_{2.5} reduction (increase) enhances (reduces) light rain frequency by +1.97 (-2.08) days yr⁻¹. Meteorological factors showed negligible temporal variability and thus insignificant explanatory power (<10% for each individual factor) over a decadal scale. Our findings establish, for the first time, the quantifiable aerosol microphysical effect on light precipitation trends, highlighting dual benefits for China's emission control policies that PM_{2.5} reduction

设置了格式: 下标

设置了格式: 下标

设置了格式: 下标

设置了格式: 下标

in 2013–2022 simultaneously enhanced light rain frequency while improving air quality. This work offers
25 critical insights for aligning air pollution mitigation with climate adaptation strategies.

1 Introduction

Precipitation serves as a pivotal physical process linking weather, climate, and the hydrological cycle. Understanding the changes in precipitation and its influence mechanisms and factors are thus of great significance. Light rain, a primary component of precipitation, is defined as precipitation with a daily
30 accumulation between 0.1 and 10 mm, [following the China Meteorological Administration \(CMA\) standard](#) (Dunkerley, 2021). Despite its relatively low intensity, the cumulative amount of light rain still accounts for a significant proportion of 20%–40% in total annual precipitation (Wang et al., 2021; Yuan et al., 2024). In addition, light rain account for more than 70% of total number of rainy days, making a significant contribution to effective precipitation in China (Fu et al., 2008; Qian et al., 2009a). Compared
35 to heavy precipitation, light rain can more easily infiltrate into the soil, and thereby plays a crucial role in maintaining soil moisture, irrigating plants, and preventing forest fires (Trenberth et al., 2003). Previously, the notable decrease in trace precipitation events or drizzle events during the years of 1950–2000 has already manifested in China (Li et al., 2008; Qian et al., 2009b). In the context of climate change and carbon emission reduction, the amount and frequency of light rain may change in China, thereby affecting
40 the climate and hydrological cycle.

In recent years, studies have analysed the characteristics and influencing factors of trends in light rain changes in China based on long-term meteorological and aerosol dataset ([Qian et al., 2009a; Jiang et al. 2014; Ma et al., 2015](#)). Research has shown that in most regions of China, particularly the eastern

regions, there has been a trend of decreasing light rain days and amounts since 1960, seasonal variations
45 have maintained the same trend as the annual average, with winter exhibiting more significant changes in
light rain days compared to other seasons (Huang and Wen, 2013; Ma et al., 2015; Wu, 2015; Zhang et
al., 2019). Although many studies have revealed the characteristics of long-term changes in light rain
days in China, it is still with big challenges to identify the driving factors. Some research have focused
on the analysing the relationship between long-term trends in meteorological factors or PM_{2.5}
50 concentrations and changes in light rain days (Fu and Dan, 2014; Wu et al., 2016; Bastin et al., 2019;
Zhang et al., 2019). Studies generally indicate that rising temperatures, increasing aerosol pollution, and
decreased relative humidity tend to suppress the occurrence of light rain (Fu and Dan, 2014; Zhou et al.,
2020; Luo et al., 2024). Lu et al. (2014) pointed out that variations and changes in rainfall total can be
dominated by changes in moisture and temperature. Studies have indicated that annual changes in the
55 number of light rain days are influenced mainly by changes in water vapor content over the eastern China
(Wu, 2015). However, it was pointed out that the correlation between large-scale water vapor transport
and light rain is not significant (Qian et al., 2009a). Statistical analysis also revealed positive correlations
between the light rain days and relative humidity (Wu et al., 2015; Zhang et al., 2019). Actually, the
decrease in relative humidity is primarily a result of rising temperature (Song et al., 2017; Zhou et al.,
60 2020). Some researchers argue that the increase in temperature reduces light rain days by affecting the
dew point temperature, as the air with the same water vapor content is more difficult to condense into
precipitation in a warmer environment than in a colder one (Qian et al., 2007). Huang et al. (Huang and
Wen, 2013; Huang et al., 2014) analysed the probable cause for the change of light rain events and
suggested that when atmospheric stability strengthens, it will promote an increase in light rain events,

65 whereas when atmospheric stability decreases, light rain events decrease. However, studies have also shown that stable atmospheric conditions are detrimental to the development of warm clouds, thereby suppressing the occurrence of light rain (Li et al., 2017).

In addition, some studies have focused on exploring the relationship between aerosol pollution and the number of light rainfall days. Aerosols can affect precipitation by serving as cloud condensation nuclei
70 (known as Aerosol-Cloud Interactions, ACIs) or by altering the radiative energy budget of the atmosphere-earth system (Aerosol-Radiation Interactions, ARIs) (Ramanathan et al., 2001; Rosenfeld et al., 2008; Li et al., 2017). Research based on observational data suggests a negative correlation in the diurnal variation of aerosols concentration and light rainfall events due to Twomey effect (Choi et al., 2008; Fu and Dan, 2014). However, a study in the TengChong area found that while the number of light
75 rainfall days showed a decreasing trend, visibility improved annually (Wu et al., 2016). Results from model simulations of aerosol effects indicate that light rainfall will decrease in heavily polluted areas, primarily due to the cloud microphysical effects of aerosols (Qian et al., 2009a; Wang et al., 2016; Shao et al., 2022), the atmospheric conditions with high aerosol loading can significantly increase the cloud droplet number concentration and reduce cloud droplet sizes compared to clean conditions. This can lead
80 to a significant decline in raindrop concentration and delay raindrop formation because smaller cloud droplets are less efficient in the collision and coalescence processes (Twomey, 1977; Qian et al., 2009a). Additionally, the increase in aerosol particles concentration has a significant impact on precipitation in China due to the aerosol radiation effect. Fan et al. (2015) found that the light rainfall was significantly suppressed in the southwestern region of China based on WRF-Chem simulation. They further showed

85 that this is may be attributed to the weakening of near-surface shortwave radiation by the aerosol radiation effect, which enhances tropospheric stability and reduces the occurrence of precipitation (Liu et al., 2022).

Overall, there remains significant uncertainty regarding the mechanisms influencing the occurrence of light rain. Most previous studies have primarily focused on the analysis of a single or very limited factors, and the relative importance of various influencing factors to the light rainfall was mostly
90 qualitatively assessed, lacking a quantitative and comprehensive evaluation. Additionally, studies on light rain days often limited to time periods when the aerosol pollution was continuously intensified in China, e.g. from around 1960s to around 2010s. A comprehensive investigation on the changes of light rainfall frequency in the most recent years of China's emission control era and its driving factors has not yet been conducted. Given the significant changes in PM_{2.5} pollution in China before and after stringent emission
95 reduction measures, as well as the background of intensified global warming and increasing number of extreme weather events, the trends and influencing factors of the light rain may undergo changes. Therefore, this study aims to obtain insights on the mechanisms affecting the changes of light rainfall days over China by combining multi datasets, multi-algorithm machine learning and causal inference modeling. The study period has been focused on the years of 2000-2022, a period during which PM_{2.5}

100 concentrations show a significant upward trajectory before 2013 followed by a markedly downward decline thereafter (see Section 3.1 and Fig. 1), providing a natural experiment to quantify aerosol effects in precipitation.~~The study period has been focused on the years of 2000-2022 when the PM_{2.5} shows an upward trajectory before 2013 followed by a markedly downward decline thereafter, providing a natural experiment to quantify aerosol effects in precipitation.~~ Section 2 presents the methods and data; In Section
105 3.1, we present the long-term variations in the light rain frequency as well as the influencing factors over

设置了格式: 下标

the studied period. In Section 3.2 & 3.3, we utilize the machine learning techniques (XGBoost and SHapley Additive exPlanations, SHAP) to quantify the importance of each individual factor to the occurrence of light rain. In Section 3.4, we discussed the key factors driving the long-term trends of the light rain frequency during the two periods. We finally incorporate Structural Equation Model (SEM) to derive insights on physical mechanisms and interactions between the various factors and the light rain occurrence.

2 Data and Methods

2.1 Data

In this study, the frequency of number of light rain days was calculated based on the dataset of CPC Global Unified Gauge-Based Analysis of Daily Precipitation (CPC-Global) (<https://psl.noaa.gov/data/g>
ridded/data.cpc.globalprecip.html). The CPC-Global dataset is with a spatial resolution of $0.5^{\circ} \times 0.5^{\circ}$ and produced based on assimilation and interpolation of observations from 30,000 stations by National Oceanic and Atmospheric Administration (NOAA) through the CPC Unified Precipitation Project (Xie et al., 2010). The daily ERA5 reanalysis data from 2000 to 2022 provided by the European Centre for Medium-range Weather Forecasts (ECMWF) was also used in this study (<https://cds.climate.copernicus.eu/>). These data include the relative humidity (RH) at 850 hpa, temperature (T) at 2 m height, the wind speed (WS) at 850 hpa, total column cloud liquid water (TCLW), low cloud cover (LCC), convective available potential energy (CAPE) and evaporation (E). The horizontal resolution for the meteorological data is 0.

25° × 0.25°. The PM_{2.5} data are obtained from the China High Air Pollutants dataset (CHAP) at a spatial
125 resolution of 1 km × 1 km from 2000 to 2022 (Wei et al., 2021, 2019; Wei, 2024).

2.2 Methods

In this study We defined the light rain event as the daily precipitation is between 0.1 and 10 mm
(Qian et al., 2009b; Huang and Wen, 2013; Wu et al., 2015) which is referenced from the standards of the
China Meteorological Administration (CMA).

130 To better demonstrate the effect of changes in PM_{2.5} and other meteorological parameters on changes
of the number of light rain days, we conducted the following analysis using data from 2000 to 2013 and
from 2013 to 2022 these two periods. The year 2013 was selected as the breakpoint because it marks a
definitive shift in China's air pollution policy with the implementation of the national "Air Pollution
Prevention and Control Action Plan", which led to a proven reversal in the long-term trend of PM_{2.5}
135 concentrations nationwide (Wei et al., 2021). The XGBoost model was applied separately to the two
periods (2000 – 2013 and 2013 – 2022) rather than to the entire dataset. This approach was chosen because
the underlying physical relationships between the predictors and light rain are expected to differ
significantly between the pollution-accumulating and pollution-abatement regimes. Training separate
models prevents the estimation of a misleading “average” relationship and allows for a more accurate
140 quantification of the distinct drivers operative in each period. Least squares technique (linear regression)
is firstly employed to estimate the annual trends of light rain days and the examined factors-(Fig. 1).
Additionally, the extreme gradient boosting (XGBoost) model is applied to examine the impact of these
factors, including PM_{2.5}, RH, WS, T, E, TCLW, CAPE, and LCC, on the number of light rain days. The

带格式的: 缩进: 首行缩进: 2 字符, 行距: 2 倍行距

设置了格式: 非上标/ 下标

selection of these specific factors is grounded in their well-established physical linkages to light rain processes, as extensively documented in prior studies (Qian et al., 2009a; Huang and Wen, 2013; Li et al., 2017). Briefly, $PM_{2.5}$ is included to quantify aerosol impacts on cloud microphysics, while the meteorological variables collectively represent the thermodynamic, moisture, dynamic, and cloud-related conditions that are fundamental to light rain formation. This approach ensures our model captures the key mechanistic drivers identified in the literature.

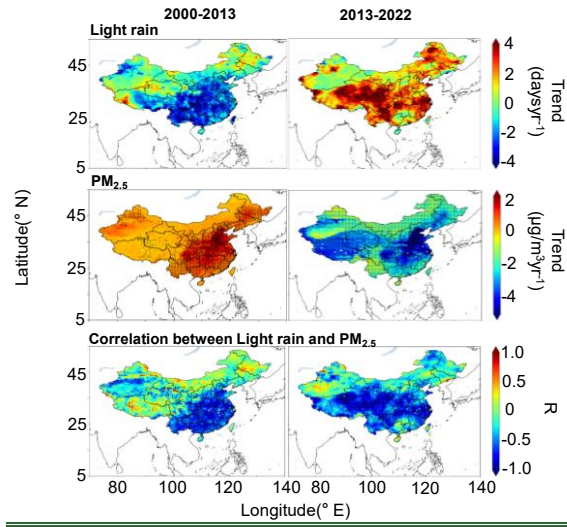


Figure 1. Spatial distribution of the trends of light rain, $PM_{2.5}$ and spatial correlation between $PM_{2.5}$ and light rain days in 2000–2013 and 2013–2022. This map of China is created based on same origin data provided by the Tianditu Platform (www.tianditu.gov.cn).

The importance of each parameter affecting the accuracy of the light rain days prediction is assessed.

The XGBoost model, which is a powerful and reliable machine learning technique, optimizes the gradient

boosted decision tree algorithm to solve regression and classification problems (Chen and Guestrin, 2016). It offers several advantages, such as handling missing values, preventing overfitting, enhancing computing speed and accuracy, and has been widely applied in predicting air pollutants and emissions (Gui et al., 2020; Si and Du, 2020, 2020). Previous studies have shown that XGBoost performs well with relatively small-scale datasets (Cheng et al., 2021; 2023). This work used 5-fold cross-validation of the training set to test the performance of the XGBoost model and defined the parameter search space to determine the optimal model parameters, finally generating the prediction results. The predicted frequency of the number of light rain days by the XGBoost method exhibit high consistency with the observed values, with mean R^2 of 0.83 and 0.90 (Fig. S3). Through K-fold cross-validation evaluation, each model achieved a mean coefficient of determination (R^2) of 0.80 on the cross-regional dataset, demonstrating robust generalization performance across different geospatial scales. Then, the drivers of the long-term variations of the light rain days over the two periods were further explored. For this, the annual trend (depicted by slope obtained based on linear fitting) of daily data for each individual factor as well as the frequency of light rain days were firstly calculated as the input variables and target parameter respectively. The result shows good performance with mean R^2 of 0.90 (Fig. S6), The K-fold cross-validation ($R^2 > 0.88$) results also demonstrate robust performance across different datasets.

~~SHapley Additive exPlanations (SHAP)~~ is a machine learning interpretability technique based on coalitional game theory (Lundberg and Lee, 2017), with its core mechanism lying in the mathematical quantification of feature contributions. Within the SHAP framework, SHAP values essentially represent a formalized mathematical deformation of Shapley values, which decompose model predictions to

attribute the deviation of each sample's predicted outcome to the contributions of individual features. The explanation could be specified as:

$$g(z') = \phi_0 + \sum_j^M \phi_j z'_j g$$

180 where g is the explanation model, $z' \in \{0,1\}^M$ is the simplified features, M is the maximum coalition size, and $\phi_j \in R$ is the weighted average of all marginal contributions for a predictor variable j , the Shapley values.

This method is particularly effective for identifying the relative importance of predictor variables in XGBoost models, providing feature attribution analysis that integrates global consistency with local
185 interpretability. Compared to feature importance methods such as the gain method or split count, SHAP not only reveals key driving factors through global importance rankings but also visualizes feature contribution distributions at the individual sample level, enabling an interpretability analysis of the interaction between model prediction and characteristic effect.

~~Structural Equation Modelling (SEM)~~ is a method that is usually used to test hypotheses on
190 relationships of multi factors within a complex system (Lamb et al., 2014; Ganjurjav et al., 2021). These hypotheses are articulated in the form of a series of regression equations, known as structural equations. This model enables the simultaneous analysis of multiple variables with causal relationships and overcomes the limitations of traditional multivariate analytical techniques such as multivariate analysis of variance and correlation analysis. When constructing an SEM, hypotheses about causal relationships
195 between variables are first formulated based on theoretical and prior research findings, and then the result is adjusted according to whether the fit indices meet statistical criteria. The key indices for evaluating SEM model fit include the Comparative Fit Index (CFI), Root Mean Square Error of Approximation

(RMSEA), and Standardized Root Mean Square Residual (SRMR). In general, when CFI approaches 1, $0 \leq RMSEA \leq 0.05$, and $0 \leq SRMR \leq 0.08$, the model indicates a very good fit (Schreiber et al., 2006, Ma et al., 2022). In addition, the chi-square test (χ^2) and Adjusted Goodness of Fit Index (AGFI) are also commonly used for model evaluation. In this study, the final model fitting results showed that CFI was 0.998 and RMSEA was 0.033, which indicates that the SEM had a very good fit with the data and that the model fit was almost ideal.

3 Results

3.1 Nationwide inverse correlation of long-term changes between aerosol concentrations and light rain frequency

Figure 1 illustrates the spatial distributions and long-term trends of light precipitation frequency and PM_{2.5} mass concentrations across China during two distinct the studied periods (2000 – 2013 and 2013 – 2022). Statistically significant decreasing trends in light rain days (mean rate: 1.0 days yr⁻¹, p < 0.05) were observed nationwide during 2000 – 2013, with the most pronounced decline in southern China (2.3 days yr⁻¹, p < 0.01) (Fig. 1a). Conversely, a reversal trend emerged during 2013 – 2022, showing continent-wide increases (1.9 days yr⁻¹, p < 0.01), particularly in southwestern China and the Yangtze River Basin (central-eastern regions), where the growth rate reached 2.6 days yr⁻¹. The data analysis Figure 1 further also reveals an inverse correlation between light precipitation trends and PM_{2.5} variations: a significant PM_{2.5} increase (0.39 µg m⁻³ yr⁻¹, p < 0.01) occurred during 2000 – 2013, contrasting with a substantial decline (2.5 µg m⁻³ yr⁻¹, p < 0.01) post - 2013. Actually, the rapid decrease in PM_{2.5} mass

设置了格式: 非突出显示

设置了格式: 非突出显示

设置了格式: 英语(英国)

带格式的: 两端对齐, 缩进: 首行缩进: 2 字符, 定义网格后不调整右缩进, 不对齐到网格

设置了格式: 英语(英国)

设置了格式: 英语(英国)

设置了格式: 英语(英国)

设置了格式: 英语(英国)

设置了格式: 英语(英国)

设置了格式: 英语(英国)

设置了格式: 字体颜色: 自动设置

设置了格式: 字体: Times New Roman, 字体颜色: 自动设置

设置了格式: 字体颜色: 自动设置

concentration since 2013 have been widely observed due to the implementation of the national “Air Pollution Prevention and Control Action Plan” in China (Zhang et al., 2020 这是我那个PNAS的文章; 其他 Ref.引用 Wei et al., 2021; Bai et al., 2024; Zhang et al., 2024). In particular, This-this inverse relationship is most evident in six anthropogenically influenced regions (Fig. 2): North China (NC), South China (SC), East China (EC), Southwest China (SWC), Central-South China (CSC), and the Fenwei Plain (FW). This regional division is based on established frameworks that consider distinct physiographic (e.g., topographic basins, climate zones) and anthropogenic (e.g., population density, industrial activity) characteristics (Chen et al., 2024). For instance, the Fenwei Plain (FW) is treated separately from North China (NC) due to its unique enclosed topography that fosters pollution accumulation, despite some similarities in overall trends.

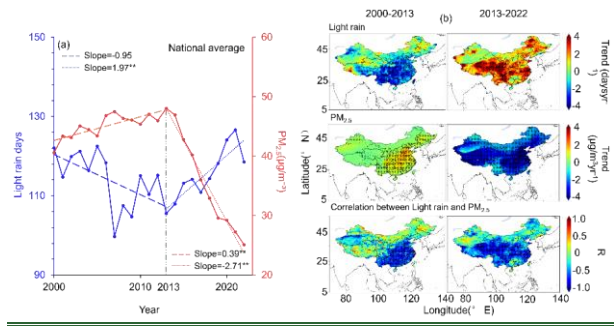


Figure 1. National trend and spatial patterns of light rain and PM_{2.5}. (a) Nationally averaged time series of light rain days (blue lines) and PM_{2.5} mass concentration (red lines) from 2000 to 2022. The dashed lines represent the piecewise linear trends for the periods 2000–2013 and 2013–2022, with the slopes indicated. Trends significant at the 95% confidence level are marked with **. (b) Spatial distribution of

设置了格式: 字体颜色: 自动设置
设置了格式: 字体颜色: 自动设置, 非突出显示
设置了格式: 字体颜色: 自动设置
设置了格式: 字体颜色: 自动设置, 非突出显示
设置了格式: 字体颜色: 自动设置
设置了格式: 英语(英国)

设置了格式: 字体: (中文)+中文正文 (等线), 小四, (中文) 简体中文(中国大陆)
设置了格式: 英语(英国)

设置了格式: 字体: 非加粗

the trends of light rain, PM_{2.5} and spatial correlation between PM_{2.5} and light rain days in 2000–2013 and 2013–2022. This map of China is created based on same-origin data provided by the Tianditu Platform (www.tianditu.gov.cn). (black dots indicate passing the 95% significance test).

Figure 1. Spatial distribution of the trends of light rain, PM_{2.5} and spatial correlation between PM_{2.5} and light rain days in 2000–2013 and 2013–2022. This map of China is created based on same-origin data provided by the Tianditu Platform (www.tianditu.gov.cn). (这里可以把全国平均的小雨变化趋势和 PM_{2.5} 变化趋势图加上，类似图 2 的那个每个区域的那个变化趋势图，这样审稿人就不会觉得我们是人为的定义了一个 turning point，我们是根据观测资料的分析结果确定的 2 个研究时段)

Since ~~P~~previous studies attribute light rain suppression in polluted regions to aerosol-cloud microphysical interactions ([Qian et al., 2009b](#); [Wang et al., 2016](#); [Shao et al., 2022](#)), ([Qian et al., 2009b](#); [Wang et al., 2016](#); [Shao et al., 2022](#)), ~~Our~~ our analysis suggests that the observed decadal shifts in light precipitation (2000 – 2013 decline vs. 2013 – 2022 increase) are likely driven by long-term aerosol concentration variability. Notably, regions with minimal anthropogenic activities (e.g., Inner Mongolia and northwestern China) exhibited no significant PM_{2.5}-light rain correlations but with good correlations with meteorological factors (e.g., RH) (Fig. 1, ~~Fig. S12~~), implying contributions from non-aerosol factors.

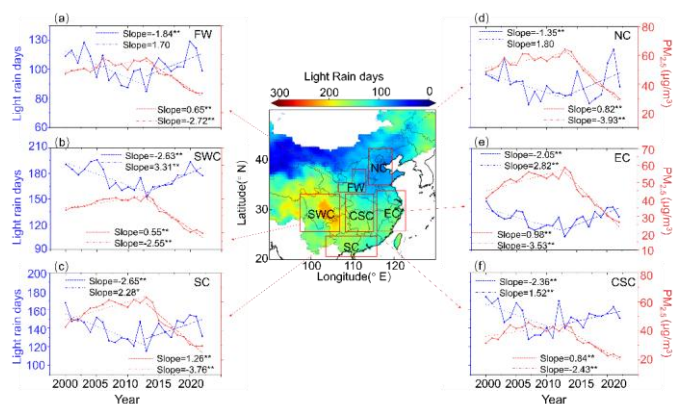


Figure 2. The fitted variation trends of light rain days (blue lines) and the fitted variation trends of PM_{2.5} (red lines) in different six selected regions. [The middle map shows the spatial distribution of average light](#)

[rain days during 2000-2022 and the six selected study regions.](#) (这个图横坐标那里还是缺“year”的 x axis information 啊)

Figure 3 depicts the long-term trends of meteorological factors (T, RH, CAPE, E, LCC, TCLW, and WS) potentially associated with light rain variability in China during 2000 – 2013 and 2013 – 2022, [while the statistical significance \(\$p < 0.05\$ \) of these trends is shown in Supplementary Fig. S1. A key observation is that, in contrast to the strong and statistically significant nationwide trends seen in PM_{2.5}, the trends of these meteorological parameters are characterized by pronounced spatial heterogeneity and largely insignificant changes over large portions of China. Clearly, spatial heterogeneity characterizes the trends of all parameters across both periods.](#) For the E, from 2000 to 2013, approximately 60% of regions exhibited insignificant trends, only with the significant decline ($p < 0.05$) observed in southwestern China and the Qinghai-Tibet Plateau (Fig. S2). During 2013 – 2022, E just decreased significantly in very few

设置了格式: 下标

~~areasaereas~~ of northeastern China and northern Xinjiang, areas concurrent with RH increases (Cong et al., 2009). Conversely, large ~~areasaereas~~ of southeastern China experienced nonsignificant E reductions. Notably, E-enhanced regions seems expanded in recent decades, likely attributable to global warming effects (IPCC, 2021). However, the enhanment is not statistically significant (Fig. S2). Analysis reveals

265 that 56% of Chinese regions showed T increases slightly during 2000 – 2013, with accelerated warming rates post - 2013. The CAPE demonstrated weakened trends across southeastern China during 2000 – 2013, while remaining stable in western/northwestern regions. This spatial pattern aligns with anthropogenic aerosol impacts. The aggravated aerosol pollution over 2000 - 2013 ~~(Fig. 1)~~ likely suppressed convection in densely populated eastern China via microphysical mechanisms (Zhao et al.,

270 2006). However, PM_{2.5} reductions since 2013 moderated CAPE declines, with some regions (e.g., middle-lower Yangtze River) even exhibiting strengthening trends, indicating meteorological sensitivity to aerosol loading changes. The TCLW decreased only in the Yangtze River Basin and Tibetan Plateau during 2000 – 2013, but reversed to increasing trends post - 2013. There are no evident variations (statistically insignificant) in TCLW elsewhere during the two periods (Fig. S2). Nationwide WS

275 reductions (statistically nonsignificant) were observed during both periods, though southeastern China experienced accelerated declines post - 2013, potentially linked to persistent particulate pollution and urbanization processes (Zhang and Wang, 2021). The RH declines affected less than 30% of China during 2000 – 2013, most prominently in the Tibetan Plateau, northeastern/southwestern China. During 2013 – 2022, it is observed with nonsignificant RH variations becoming dominant nationwide. The LCC trends

280 spatially mirrored RH patterns, likely underscoring their coupled responses to anthropogenic and climatic drivers. While these meteorological parameters exhibited spatially variable trends, their magnitudes were

generally much smaller than PM_{2.5} variations. Subsequent sections will quantitatively evaluate their combined impacts on light rain frequency.

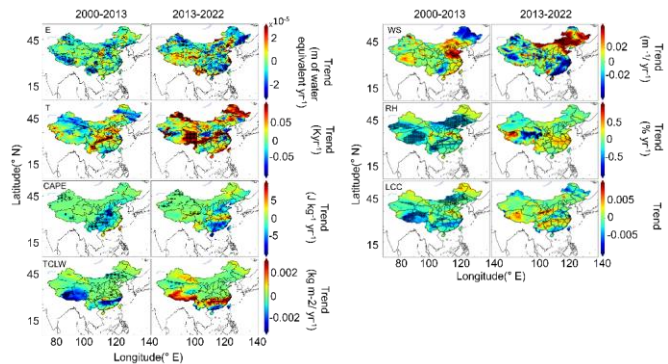


Figure 3. The fitted variation trends of other affecting factors of ~~evaporation (E), temperature (T), Convective Available Potential Energy (CAPE), total cloud liquid water (TCLW), wind speed (WS) relative humidity (RH), and low cloud cover (LCC)~~ of China over 2000 - 2013 and 2013 - 2022.

3.2 Quantifying the relative contributions of individual factors to light precipitation events

To elucidate the influence of aerosols and meteorological parameters on light precipitation events, variable importance metrics were derived using the machine learning - based XGBoost algorithm. Considering that the temporal variation trends of these factors are not identical, we presented and analyzed the conditions of the two research periods (2000–2013 and 2013–2022) (Fig. 4) – this was done to compare and explore whether the relative contribution or importance of each factor to precipitation has changed across different stages. during 2000–2013 and 2013–2022. The XGBoost-based model demonstrates robust predictive capability, achieving a correlation coefficient of 0.83 and 0.90 (Slope:

0.80, 0.85 $p < 0.01$) between predicted and observed light precipitation events (Fig. S3). This validation ensures the reliability of subsequent parameter importance evaluations for elucidating meteorological drivers of light rain. Figure 4 quantifies the relative contributions of the $PM_{2.5}$ and meteorological factors (RH, T, E, TCLW, CAPE, LCC, WS) to light rain occurrence during 2000 – 2013 and 2013 – 2022.

300 Nationwide, ~~relative humidity (RH)~~ exerted the dominant influence, accounting for 32% of light rain variability across both periods. The $PM_{2.5}$, ~~temperature (T)~~, and ~~evaporation (E)~~ followed as key drivers, with mean contributions of 15.5%/11.7%/11.7% in 2000 – 2013 and 12.1%/10.5%/11.5% in 2013 – 2022 respectively. Notably, the contribution of $PM_{2.5}$ declined significantly from 15.5% to 12.1% (a 3.4% decrease, $p < 0.05$)~~relative importance of the $PM_{2.5}$ declined by 3.4% post 2013 ($p < 0.05$)~~, coinciding
305 with China's stringent emission controls (Shao et al., 2022; Wang et al., 2016). Conversely, the contributions of TCLW and CAPE increased significantly from 7.2%/9.4% in 2000 – 2013 to 13.6%/10.6% in 2013 – 2022 ($p < 0.01$). LCC and WS remained negligibly minor factors ($< 6\%$ contribution). Moreover, spatial heterogeneity (Fig. 3) revealed no substantial differences in factor contributions between the two periods, except for $PM_{2.5}$ and TCLW. Conspicuously, the meteorological factors exhibited statistically
310 insignificant temporal trends (~~Fig. 3~~), implying stable physical mechanisms underlying their impacts on light rain.

设置了格式: 下标

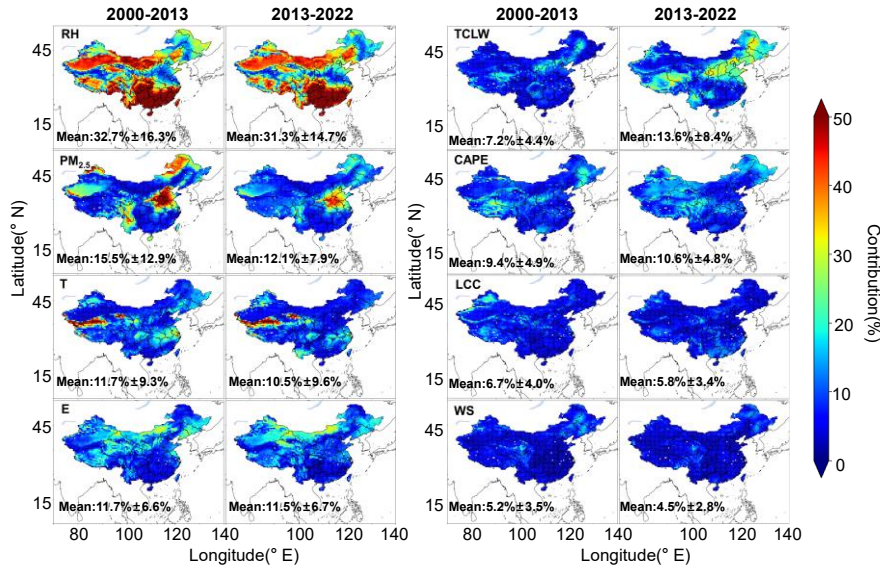


Figure 4. The relative contribution of ~~relative humidity (RH)~~, ~~PM_{2.5} mass concentration~~, ~~temperature (T)~~, ~~evaporation (E)~~, ~~total cloud liquid water (TCLW)~~, ~~convective available potential energy (CAPE)~~, ~~low cloud cover (LCC)~~ and ~~wind speed (WS)~~ to light rain events over 2000 - 2013 and 2013 - 2022.

Spatial heterogeneity characterizes the relative importance of meteorological factors (Fig. 5). For instance, the RH exerts critical influence in southeastern and northwestern China, peaking at 50% contribution in southern regions. This spatial pattern aligns with established findings showing significant RH - light rain day correlations in southern China (Wu et al., 2015; S. Zhang et al., 2019; Zhou et al., 2020). Conversely, the contribution of RH diminishes to ~10% in northern regions, likely attributable to lower atmospheric moisture content (Fig. 5b). In contrast, PM_{2.5} emerges as the dominant driver in northern China, especially in North China Plain (NCP), where aerosol concentrations exceed those in

pristine western regions (Fig. S4). This aerosol-mediated regulation aligns with cloud microphysical mechanisms suppressing light precipitation (Qian et al., 2009b; Yang et al., 2016). The E demonstrates pronounced influence in arid Inner Mongolia and northwestern China, consistent with hydrological sensitivity in water - limited ecosystems (Chen Yaning et al., 2014; Yang Yaqing et al., 2024). The E - light rain relationship weakens eastward, reflecting enhanced soil moisture buffering in humid regions. The TCLW assumes greater significance in western and northeastern China, where the water vapor content is relatively low, the warm cloud precipitation process, which relies on the growth of liquid water and the collision and coalescence of water droplets, makes the TCLW a crucial factor for the occurrence of light rain (Gao et al., 2016). Notably, importance of TCLW increased significantly (+ 18%) in NCP and northeastern China post - 2013, coinciding with PM_{2.5} reductions that reduced cloud condensation nuclei (CCN) and elevated cloud droplet coalescence efficiency (Twomey, 1977; Guo et al., 2019). Consequently, even small changes in TCLW can directly reflect the occurrence of light rain. These findings underscore the complexity of regional meteorological controls, necessitating regionalized analyses for mechanistic correlation.

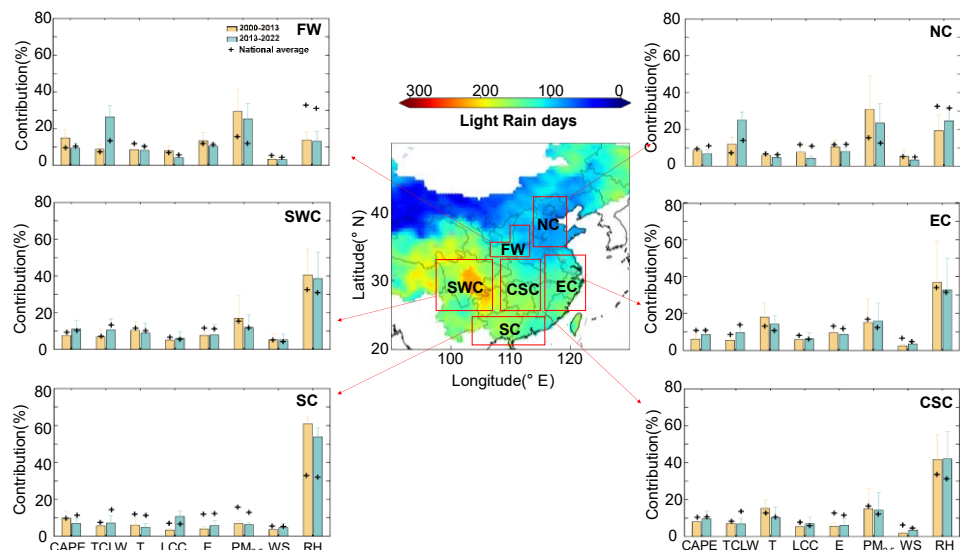


Figure 5. Comparison of the contribution of individual factors to light rain events over 2000 - 2013 and 2013 - 2022 in the selected six regions of China.

3.3 Comparison of the relative contributions of individual factors to light precipitation events in selected regions of China

The analysis is further conducted in the six typical areas with elevated anthropogenic emissions. As shown in Fig. 5, there are large differences in the dominant factors affecting light rain frequency across regions. The RH plays a leading role in SC, EC, SWC, and CSC regions, with mean contributions of ~40%. In FW and NC regions, RH contributions diminish to 15–20%, whereas $PM_{2.5}$ contributions increase markedly (20–30%), exceeding the national average by approximately twofold. This anthropogenic imprint is amplified in other high-emission regions (CSC, SWC, EC), where $PM_{2.5}$ exhibits

considerable influence. Other factors (CAPE, WS, T, E, LCC) show no substantial variations in contributions (< 10%) across the six regions. These findings indicate the dominant role of anthropogenic emissions in light rain occurrence within heavily polluted areas. Notably, impact of PM_{2.5} declined slightly in NC and FW during 2013 – 2022 compared to 2000 – 2013, aligning with China's pollution controls. The declines are consistent with decreases in the national average but showing steeper reductions. Concurrently, TCLW gained prominence in most regions (except CSC) post - 2013, increasing its contribution to near 30%. These results underscore aerosol-cloud microphysical effects as critical regulators of light precipitation in polluted regions.

3.4 Factors and mechanisms that drive the long-term trends of light rain frequency

To elucidate the drivers of long-term trends in light rain day frequency ~~described in Section 3.1 (Figs. 1, 2)~~, we systematically investigated the relative contributions of multi-factors using an integrated machine learning (XGBoost), interpretability technique (SHAP) and ~~structural equation modeling (SEM)~~ framework (Fig. 6). As stated previously, considering that the temporal variation trends of these factors are not identical, we presented and analysed the conditions of the two research periods (2000–2013 and 2013–2022) – this was done to compare and explore whether the driving factors of influencing the precipitation long-term trends has changed across different stages. Therefore, this dual-method approach quantifies both observed patterns (e.g., downward trends in 2000–2013 vs. upward trends post - 2013) and underlying causal mechanisms. The results show good performance of our established model for predicting the trends of light rain frequency (with correlation coefficient $R^2=0.90$ between the measured and predicted trends of light rain frequency) (Fig. S5).

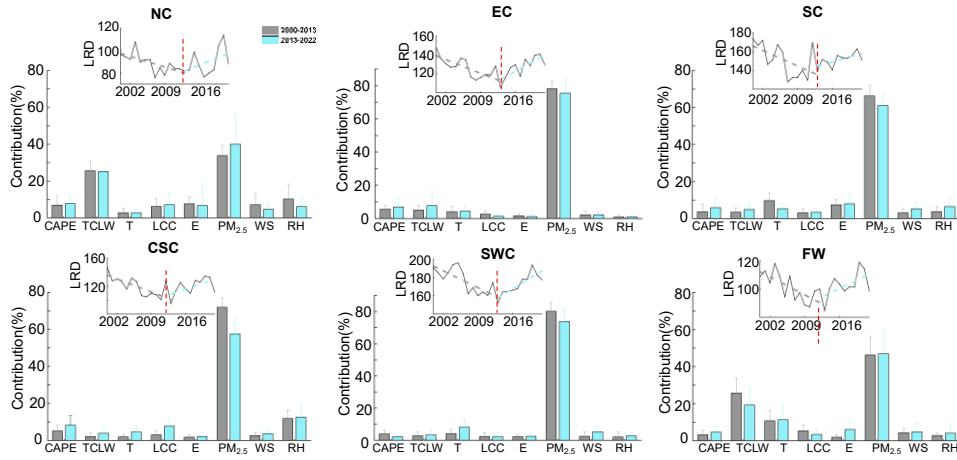


Figure 6. Factors that drive the long-term trends of light rain frequency in the selected six regions of

China. The small graphs embedded in the middle are the average trends of light rain frequency over 2000 - 2022 in the six regions, and the grey lines represent the fitted trend of light rain days from 2000 to 2013, while the blue lines depict the fitted trend for the period of 2013 - 2022.

The results demonstrate aerosol dominant role in driving long-term trends in light precipitation frequency across both periods, contributing ~~59.8~~^{63.5}% to the interannual variability of annual light rain days (Fig. 6). Specifically, the increasing trend in PM_{2.5} concentrations in 2000 - 2013 has led to varying magnitudes of decreases in the number of light rain days in the six regions, 0.65 days yr⁻¹ (NC), 2.22 days yr⁻¹ (EC), 1.64 days yr⁻¹ (SC), 2.04 days yr⁻¹ (CSC), 3.0 days yr⁻¹ (SWC), and 1.0 days yr⁻¹ (FW). (Fig. 7). Conversely, the pronounced decrease in PM_{2.5} levels from 2013 to 2022 has increased the light rain days of 0.7 days yr⁻¹ (NC), 2.42 days yr⁻¹ (EC), 1.66 days yr⁻¹ (SC), 1.85 days yr⁻¹ (CSC), 2.62 days yr⁻¹ (SWC), and 1.0 days yr⁻¹ (FW) (Fig. 7). Note that, compared to the period of 2000 - 2013, the relative

importance of the variations in PM_{2.5} in affecting the light rain in recent years of 2013 - 2022 becomes more prominent likely associated with the rapid nationwide decrease of aerosol concentrations since 2013. This aligns with Twomey's cloud albedo effect (Twomey, 1977), where elevated aerosol loadings suppress light precipitation via cloud microphysical feedbacks (Qian et al., 2009b; Wang et al., 2016; Shao et al., 2022). Reduced aerosol concentrations post - 2013 attenuated these suppression effects, enhancing light rain frequency through improved cloud droplet coalescence efficiency. Machine learning-based analysis further elucidates this underlying microphysical aerosol-mediated mechanism (Figs. 6,7), revealing aerosols dominant influence on light precipitation. These findings reconcile national-scale aerosol-light rain described in Section 3.1~~decoupling trends (shown in Figs. 1,2)~~ with microphysical process dynamics. Averaging the regional results from Fig. 7, the national mean contribution of PM_{2.5} was -2.08 days yr⁻¹ during 2000-2013 and +1.97 days yr⁻¹ during 2013-2022.

设置了格式: 下标

设置了格式: 上标

设置了格式: 上标

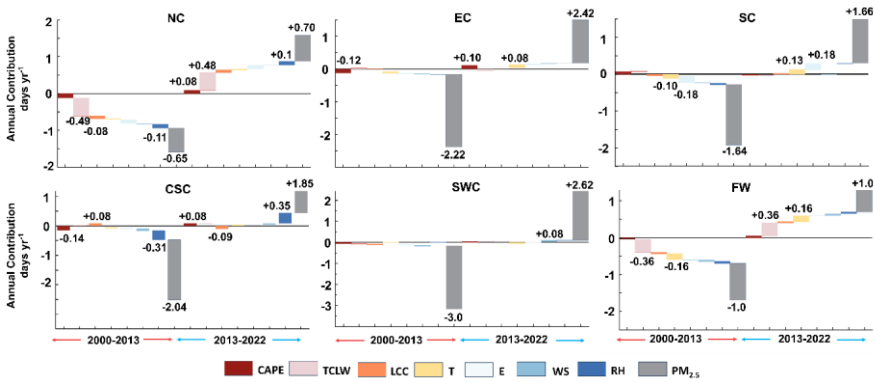


Figure 7. Quantified contribution of each factor~~Quantified contribution of each individual factor~~ to the long-term changes of light rain days in the six selected regions of China over the periods of 2000 - 2013 and 2013 - 2022. (这个图不对，两个时间段不是标在 NC 那个图，你们按照最新版本修改)

Other meteorological factors, such as RH and LCC, demonstrated significant positive correlations with light rain day frequency in most regions (Figs. S7-11). Our trend analysis in Section 3.1 revealed that they, along with the new insights from regional analysis (Fig. 8), exhibited statistically insignificant long-term changes over the study period. Consequently, their quantified contributions to interannual variability
 400 were negligible (<10%), further supporting the conclusion that aerosols were the dominant driver of the observed trend reversal. However, these factors exhibited non-significant long-term trends across all periods (Figs. 3, 8, Fig. S2), with negligible contributions (< 10%) to interannual variability (Figs. 6, 7).
 Notably, in NC, the TCLW showed considerable importance in regulating the long-term variations of light rain frequency, explaining 26% of light rain days decline (about - 0.49 days yr⁻¹) over 2000 - 2013
 405 and 25% of the light rain increase (about + 0.48 days yr⁻¹) during 2013 - 2022. Similar patterns were observed in FW, likely attributable to shared climatic and pollution regimes between these two northern regions.

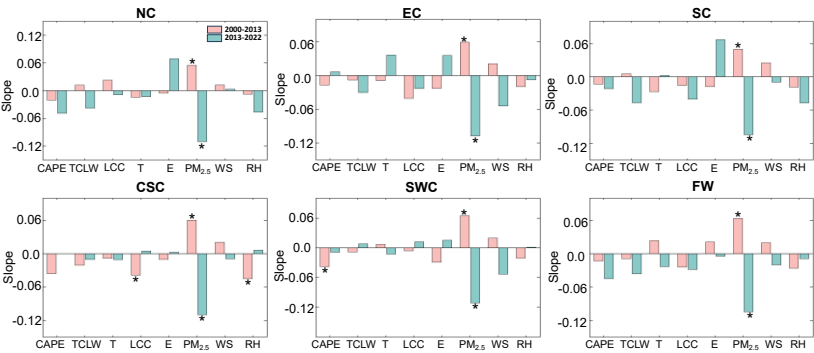


Figure 8. The regional average long-term trends of each individual factor in the selected six regions of
 410 China. The black asterisk (*) represent the fitted trend that passes the significance test.

4 Discussion and conclusion

To systematically validate our findings, we conducted supplementary analyses using SHAP and ~~structural equation modeling (SEM)~~ (Figs. 9-10). Results consistently demonstrate that PM_{2.5} long-term trends exert the most critical influence on light rain day variability across the six regions. Notably, negative SHAP values (− 0.40 to − 3.82, depending on regional variations) emerge under elevated PM_{2.5} concentrations (> 40 µg m^{−3}), indicating aerosol-mediated suppression of light precipitation via cloud microphysical feedbacks (Twomey, 1977). Conversely, positive SHAP values (+ 0.38 to + 3.48) correspond to PM_{2.5} reductions (< 30 µg m^{−3}), reflecting enhanced light rain frequency through improved cloud droplet coalescence efficiency. These findings corroborate XGBoost-derived conclusions, reinforcing the robustness of aerosol-driven mechanisms in light precipitation regulation. The SEM analysis further corroborates aerosols direct suppression effect on light rain frequency, demonstrating a significant negative correlation ($r = -0.29$, $p < 0.01$; Fig. 10). SEM also elucidates indirect pathways through which PM_{2.5} modulates precipitation by altering key meteorological factors. For example, PM_{2.5} exhibits an inverse correlation with total column water vapor (TCLW; $r = -0.23$, $p < 0.05$), indicating aerosol-mediated cloud liquid water reduction (Fig. 10). Mechanistically, elevated aerosols reduce TCLW through two synergistic pathways, firstly, the increased aerosols enhanced cloud droplet evaporation due to radiative heating (the semi-direct effect) (Hansen et al., 1997; Johnson et al., 2004; Huang et al., 2014; Fan et al., 2015); second, Elevated aerosol loading can reduce TCLW by enhancing cloud-top radiative cooling and turbulent entrainment, which introduce dry air into the cloud, promote droplet evaporation, and decrease cloud water content (Wang et al., 2003; Ackerman et al., 2004; Bretherton et al., 2007; Xue et al., 2008; Williams and Igel, 2021; Fons et al., 2023). In addition, increased aerosol concentrations

suppress evaporation (E; $r = -0.14$, $p < 0.05$), reflecting radiative cooling effects that reduce atmospheric moisture (Niu et al., 2010). These combined effects diminish liquid water accumulation and cloud droplet growth, ultimately suppressing light precipitation. Furthermore, SEM reveals aerosols-RH coupling interaction ($r = -0.42$, $p < 0.001$), confirming aerosols dual regulatory roles in direct microphysical suppression and indirect climatic feedbacks.

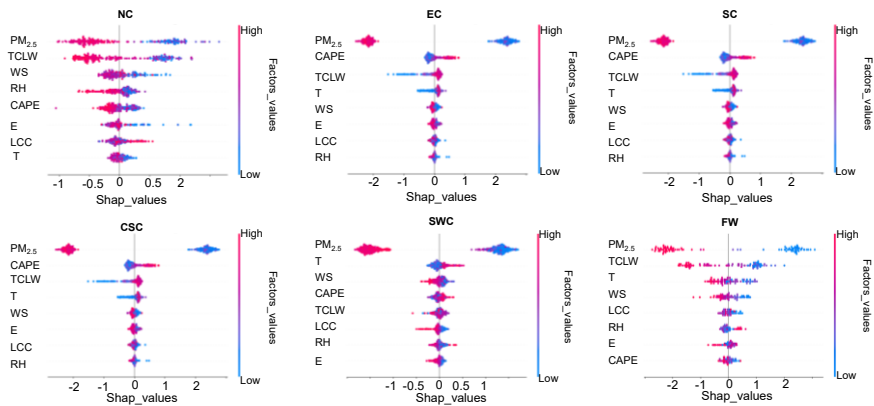


Figure 9. The SHAP values of each individual factor to the long-term trends of light rain days in the six selected regions of China.

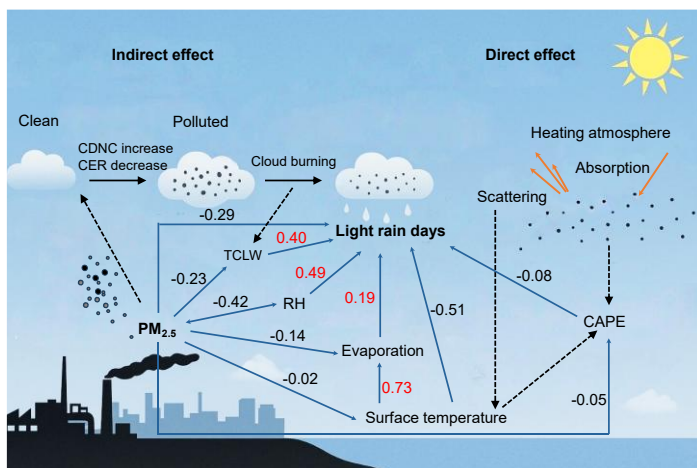


Figure 10. Structural equation model (SEM) to determine the effects of factors on light rain days. The numbers next to the arrows represent normalized path coefficients. All the paths' coefficients in the model were highly significant ($p < 0.001$).

Note that, the SEM analysis demonstrates a significant positive correlation between TCLW and precipitation ($r = 0.41$, $p < 0.01$) (Fig. 10). While in highly polluted regions (e.g., NC and FW), elevated TCLW values exhibit negative SHAP values, suggesting aerosol-mediated suppression of light precipitation. This inverse relationship may stem from enhanced convective precipitation efficiency under extreme aerosol loading in northern China (Li et al., 2011), where cloud water is preferentially partitioned into precipitation rather than sustaining liquid water accumulation. Conversely, in other regions, TCLW increases correlate positively with light rain frequency, which is in accordance with the results of previous studies (Liu et al., 2011; Wu et al., 2017; Y. Zhang et al., 2019) indicating distinct aerosol thresholds governing cloud microphysical processes. These findings also align with the mechanism proposed by (Zhang et al., 2019). Further analysis reveals that models constructed with warm-season data demonstrate

455 robust performance (Figs. S12.13), with prediction outcomes exhibiting high consistency with those
derived from annual datasets. This finding validates, at a seasonal scale, the cross-seasonal stability of
PM_{2.5} concentration impact on light rainfall frequency (Figs. S14 - 17).

In conclusion, our long-term observational analysis (2000 – 2022~~3~~) reveals a declining trend in light
rain occurrences (-1.0 days yr^{-1} , $p < 0.05$) during 2000–2013, followed by a significant reversal to
460 increasing trends ($+1.9$ days yr^{-1} , $p < 0.01$) post - 2013. This decadal shift exhibits an inverse correlation
between aerosol loading and light rain frequency across China, consistent with anthropogenic aerosol
impacts on cloud microphysics. Machine learning (XGBoost-SHAP) and ~~structural equation modeling~~
(SEM) jointly demonstrate aerosol's dominant role in driving these trends, with mechanistic insights into
cloud droplet coalescence suppression. Meteorological factors (RH, LCC) show non-significant
465 interannual variability ($\Delta < 0.1$ days yr^{-1} , $p > 0.1$), indicating negligible contributions to light rain
variability over a decade scale. The study reveals dual benefits of China's emission reduction measures
on improving air quality and responding to extreme precipitation weather. Despite our model yielding
new insights into the aerosols role in affecting the long-term changes of light rainfall in China, there
remain uncertainties due to limitations in the model algorithms, variable selection and data resolution. In
470 future work, consideration can be given to incorporating more variables and utilizing different reanalysis
datasets to improve the model performance.

Data availability. Data are available from the following sites: CPC-global, <https://psl.noaa.gov/data/grid>
[ded/data.cpc.globalprecip.html](https://psl.noaa.gov/data/grid); ERA5, <https://www.ecmwf.int/en/forecasts/dataset/ecmwf-reanalysis-v5>;
475 CHAP, <https://zenodo.org/records/6398971>

Code availability. All code is available upon <https://github.com/TK-0908/>

Declaration of competing interest. The authors declare no competing interests.

Author contributions. FZ and RZ conceived the conceptual development of the manuscript. LC directed experiments and RZ performed the experiments with PW, GL and XH, and FZ and RZ conducted the data analysis and wrote the draft of the manuscript, and all authors edited and commented on the various sections of the manuscript.

Acknowledgments. This work was funded by the National Natural Science Foundation of China (NSFC) research project (Grant No. 42475112), Shenzhen Science and Technology Plan Project (Grant No. GXWD20220811174022002; KCXST20221021111404011), Guangdong Natural Science Foundation (Grant No. 2024A1515011005).

References

Ackerman, A.S., Kirkpatrick, M.P., Stevens, D.E., Toon, O.B.: The impact of humidity above stratiform clouds on indirect aerosol climate forcing, *Nature*, 432, 1014–1017, <https://doi.org/10.1038/nature03174>, 2004.

IPCC: AR6 Synthesis Report: Climate Change 2023, Intergovernmental Panel on Climate Change, 2023, <https://www.ipcc.ch/report/ar6/syr/>, last access: 5 February 2025.

Bai, Y., Liu, M.: Multi-scale spatiotemporal trends and corresponding disparities of PM2.5 exposure in China. *Env. pollution*, 340, 122857. <https://doi.org/10.1016/j.envpol.2023.122857>, 2024.

Bastin, S., Drobinski, P., Chiriaco, M., Bock, O., Roehrig, R., Gallardo, C., Conte, D., Domínguez Alonso, M., Li, L., Lionello, P., Parracho, A.C.: Impact of humidity biases on light precipitation occurrence: observations versus simulations, *Atmos. Chem. Phys.*, 19, 1471–1490, <https://doi.org/10.5194/acp-19-1471-2019>, 2019.

Bretherton, C.S., Blossey, P.N., Uchida, J.: Cloud droplet sedimentation, entrainment efficiency, and subtropical stratocumulus albedo, *Geophys. Res. Lett.*, 34, <https://doi.org/10.1029/2006GL027648>, 2007.

Chen, L., Zhang, F., Ren, J., Li, Z., Xu, W., Sun, Y., Liu, L., Wang, X.: Changes in wintertime visibility across China over 2013–2019 and the drivers: A comprehensive assessment using machine learning method. *Sci. Total Environ.*, 912, 169516. <https://doi.org/10.1016/j.scitotenv.2023.169516>, 2024.

Chen, T., Guestrin, C.: XGBoost: A Scalable Tree Boosting System, in: KDD '16: Proceedings of the 22nd ACM SIGKDD International Conference on Knowledge Discovery and Data Mining, 785–794. <https://doi.org/10.1145/2939672.2939785>, 2016.

Chen, Y., Li, Z., Fan, Y., Wang, H., Fang, G.: Research progress on the impact of climate change on water resources in the arid region of Northwest China, *Acta Geographica Sinica*, 69, 1295–1304, <https://doi.org/10.11821/dlxb201409005>, 2014.

设置了格式: 字体: 10 磅, 英语(美国)

- Cheng, Y., Huang, X., Peng, Y., Tang, M., Zhu, B., Xia, S., He, L.: A novel machine learning method for evaluating the impact of emission sources on ozone formation, *Environ. Pollut.*, 316, 120685, <https://doi.org/10.1016/j.envpol.2022.120685>, 2023.
- 510 Cheng, Y., Zhu, Q., Peng, Y., Huang, X., He, L.: Multiple strategies for a novel hybrid forecasting algorithm of ozone based on data-driven models, *J. Cleaner Prod.*, 326, 129451, <https://doi.org/10.1016/j.jclepro.2021.129451>, 2021.
- Choi, Y., Ho, C., Kim, J., Gong, D., Park, R.J.: The Impact of Aerosols on the Summer Rainfall Frequency in China, *J. Appl. Meteorol. Climatol.*, 47, 1802–1813, <https://doi.org/10.1175/2007JAMC1745.1>, 2008.
- 515 Cong, Z., Yang, D., Ni, G.: Does evaporation paradox exist in China?, *Hydrol. Earth Syst. Sci.*, 13, 357–366, <https://doi.org/10.5194/hess-13-357-2009>, 2009.
- Dunkerley, D. L.: Light and low-intensity rainfalls: A review of their classification, occurrence, and importance in landsurface, ecological and environmental processes, *Earth-Sci. Rev.*, 214, 103529, <https://doi.org/10.1016/j.earscirev.2021.103529>, 2021.
- 520 Fan, J., Rosenfeld, D., Yang, Y., Zhao, C., Leung, L. R., Li, Z.: Substantial contribution of anthropogenic air pollution to catastrophic floods in Southwest China: AIR POLLUTION TO CATASTROPHIC FLOODS, *Geophys. Res. Lett.*, 42, 6066–6075, <https://doi.org/10.1002/2015GL064479>, 2015.
- Fons, E., Runge, J., Neubauer, D., Lohmann, U.: Stratocumulus adjustments to aerosol perturbations disentangled with a causal approach, *npj Clim. Atmos. Sci.*, 6, 130, <https://doi.org/10.1038/s41612-023-00452-w>, 2023.
- 525 Fu, C., Dan, L.: Trends in the different grades of precipitation over South China during 1960–2010 and the possible link with anthropogenic aerosols, *Adv. Atmos. Sci.*, 31, 480–491, <https://doi.org/10.1007/s00376-013-2102-7>, 2014.
- Fu, J., Qian, W., Lin, X., Chen, D.: Trends in graded precipitation in China from 1961 to 2000, *Adv. Atmos. Sci.*, 25, 267–278, <https://doi.org/10.1007/s00376-008-0267-2>, 2008.
- Ganjurjav, H., Gornish, E., Hu, G., Wu, J., Wan, Y., Li, Y., Gao, Q.: Phenological changes offset the warming effects on biomass production in an alpine meadow on the Qinghai–Tibetan Plateau, *J. Ecol.*, 109, 1014–1025, <https://doi.org/10.1111/1365-2745.13531>, 2021.
- 530 Gao, W., Sui, C., Fan, J., Hu, Z., Zhong, L.: A study of cloud microphysics and precipitation over the Tibetan Plateau by radar observations and cloud-resolving model simulations, *J. Geophys. Res. Atmos.*, 121, 13735–13752, <https://doi.org/10.1002/2015JD024196>, 2016.
- 535 Gui, K., Che, H., Zeng, Z., Wang, Y., Zhai, S., Wang, Z., Luo, M., Zhang, L., Liao, T., Zhao, H., Li, L., Zheng, Y., Zhang, X.: Construction of a virtual PM_{2.5} observation network in China based on high-density surface meteorological observations using the Extreme Gradient Boosting model, *Environ. Int.*, 141, 105801, <https://doi.org/10.1016/j.envint.2020.105801>, 2020.
- Guo, J., Su, T., Chen, D., Wang, J., Li, Z., Lv, Y., Guo, X., Liu, H., Cribb, M., Zhai, P.: Declining Summertime Local-Scale Precipitation Frequency Over China and the United States, 1981–2012: The Disparate Roles of Aerosols, *Geophys. Res. Lett.*, 46, 13281–13289, <https://doi.org/10.1029/2019GL085442>, 2019.
- 540 Hansen, J., Sato, M., Ruedy, R.: Radiative forcing and climate response, *J. Geophys. Res. Atmos.*, 102, 6831–6864, <https://doi.org/10.1029/96JD03436>, 1997.
- Huang, G., Wen, G.: Spatial and temporal variations of light rain events over China and the mid-high latitudes of the Northern Hemisphere, *Chin. Sci. Bull.*, 58, 1402–1411, <https://doi.org/10.1007/s11434-012-5593-1>, 2013.
- 545 Huang, J., Wang, T., Wang, W., Li, Z., Yan, H.: Climate effects of dust aerosols over East Asian arid and semiarid regions, *J. Geophys. Res. Atmos.*, 119, 11398–11416, <https://doi.org/10.1002/2014JD021796>, 2014.
- [Jiang, Z., Shen, Y., Ma, T., Zhai, P., Fang, S.: Changes of precipitation intensity spectra in different regions of mainland China during 1961–2006. *J Meteorol Res*, 28, 1085–1098, <https://doi.org/10.1007/s13351-014-3233-1>, 2014.](#)
- 550 Johnson, B. T., Shine, K. P., Forster, P. M.: The semi-direct aerosol effect: Impact of absorbing aerosols on marine stratocumulus, *Q. J. R. Meteorol. Soc.*, 130, 1407–1422, <https://doi.org/10.1256/qj.03.61>, 2004.
- Lamb, E. G., Mengersen, K. L., Stewart, K. J., Attanayake, U., Siciliano, S. D.: Spatially explicit structural equation modeling, *Ecology*, 95, 2434–2442, <https://doi.org/10.1890/13-1997.1>, 2014.
- Li, H., Zhou, T., Yu, R.: Analysis of July–August Daily Precipitation Characteristics Variation in Eastern China during 1958–2000, *Chinese J. Atmos. Sci.*, 32, 358–370, <https://doi.org/10.3878/j.issn.1006-9895.2008.02.14>, 2008.
- 555 Li, Z., Niu, F., Fan, J., Liu, Y., Rosenfeld, D., Ding, Y.: Long-term impacts of aerosols on the vertical development of clouds and precipitation, *Nat. Geosci.*, 4, 888–894, <https://doi.org/10.1038/ngeo1313>, 2011.

- Li, Z., Rosenfeld, D., Fan, J.: Aerosols and Their Impact on Radiation, Clouds, Precipitation, and Severe Weather Events, in: Oxford Research Encyclopedia of Environmental Science, Oxford University Press, <https://doi.org/10.1093/acrefore/9780199389414.013.126>, 2017.
- 560 Liu, B., Xu, M., Henderson, M.: Where have all the showers gone? Regional declines in light precipitation events in China, 1960-2000, *Int. J. Climatol.*, 31, 1177–1191, <https://doi.org/10.1002/joc.2144>, 2011.
- Liu, J., Zhao, C., Lin, Y., Zhang, Q., Liu, H., Xiao, Q., Peng, Y.: Potential Impacts of Aerosol on Diurnal Variation of Precipitation in Autumn Over the Sichuan Basin, China, *J. Geophys. Res.-Atmos.*, 127, e2022JD036674, <https://doi.org/10.1029/2022JD036674>, 2022.
- 565 Lu, E., Zeng, Y., Luo, Y., Ding, Y., Zhao, W., Liu, S., Gong, L., Jiang, Y., Jiang, Z., Chen, H.: Changes of summer precipitation in China: The dominance of frequency and intensity and linkage with changes in moisture and air temperature, *J. Geophys. Res.-Atmos.*, 119, <https://doi.org/10.1002/2014JD022456>, 2014.
- Lundberg, S., Lee, S. I.: A Unified Approach to Interpreting Model Predictions, *Adv. Neural Inf. Process. Syst.*, <https://doi.org/10.48550/arXiv.1705.07874>, 2017.
- 570 Luo, F., Wang, S., Wang, H., Shu, X., Huang, J.: Differing Contributions of Anthropogenic Aerosols and Greenhouse Gases on Precipitation Intensity Percentiles Over the Middle and Lower Reaches of the Yangtze River, *J. Geophys. Res.-Atmos.*, 129, e2023JD040202, <https://doi.org/10.1029/2023JD040202>, 2024.
- Ma, S., Zhou, T., Dai, A., Han, Z.: Observed Changes in the Distributions of Daily Precipitation Frequency and Amount over China from 1960 to 2013, *J. Climate*, 28, 6960–6978, <https://doi.org/10.1175/JCLI-D-15-0011.1>, 2015.
- 575 [Ma, W., Ding, J., Wang, J., & Zhang, J.: Effects of aerosol on terrestrial gross primary productivity in Central Asia. *Atmos. Environ.* 288, 119294. <https://doi.org/10.1016/j.atmosenv.2022.119294>, 2022.](#)
- Qian, W., Fu, J., Yan, Z.: Decrease of light rain events in summer associated with a warming environment in China during 1961–2005, *Geophys. Res. Lett.*, 34, <https://doi.org/10.1029/2007GL029631>, 2007.
- Qian, Y., Gong, D., Fan, J., Leung, L. R., Bennartz, R., Chen, D., Wang, W.: Heavy pollution suppresses light rain in China: Observations and modeling, *J. Geophys. Res.*, 114, D00K02, <https://doi.org/10.1029/2008JD011575>, 2009a.
- 580 Qian, Y., Gong, D., Fan, J., Leung, L. R., Bennartz, R., Chen, D., Wang, W.: Heavy pollution suppresses light rain in China: Observations and modeling, *J. Geophys. Res.*, 114, D00K02, <https://doi.org/10.1029/2008JD011575>, 2009b.
- Ramanathan, V., Crutzen, P. J., Kiehl, J. T., Rosenfeld, D.: Aerosols, Climate, and the Hydrological Cycle, *Science*, 294, 2119–2124, <https://doi.org/10.1126/science.1064034>, 2001.
- 585 Rosenfeld, D., Lohmann, U., Raga, G. B., O'Dowd, C. D., Kulmala, M., Fuzzi, S., Reissell, A., Andreae, M. O.: Flood or Drought: How Do Aerosols Affect Precipitation?, *Science*, 321, 1309–1313, <https://doi.org/10.1126/science.1160606>, 2008.
- [Schreiber, J. B., Nora, A., Stage, F. K., Barlow, E. A., & King, J.: Reporting Structural Equation Modeling and Confirmatory Factor Analysis Results: A Review. *Int. J. Educ. Res.* 99\(6\), 323–338. <https://doi.org/10.3200/JOER.99.6.323-338>, 2006.](#)
- 590 Shao, T., Liu, Y., Wang, R., Zhu, Q., Tan, Z., Luo, R.: Role of anthropogenic aerosols in affecting different-grade precipitation over eastern China: A case study, *Sci. Total Environ.*, 807, 150886, <https://doi.org/10.1016/j.scitotenv.2021.150886>, 2022.
- Si, M., Du, K.: Development of a predictive emissions model using a gradient boosting machine learning method, *Environ. Technol. Innov.*, 20, 101028, <https://doi.org/10.1016/j.eti.2020.101028>, 2020.
- 595 Song, S., Jing, C., Hu, Z.: Opposite Trends in Light Rain Days over Western and Eastern China from 1960 to 2014, *Atmosphere*, 8, 54, <https://doi.org/10.3390/atmos8030054>, 2017.
- Trenberth, K. E., Dai, A., Rasmussen, R. M., Parsons, D. B.: The Changing Character of Precipitation, *Bull. Amer. Meteorol. Soc.*, 84, 1205–1218, <https://doi.org/10.1175/BAMS-84-9-1205>, 2003.
- 600 Twomey, S.: The Influence of Pollution on the Shortwave Albedo of Clouds, *J. Atmos. Sci.*, 34, 1149–1152, [https://doi.org/10.1175/1520-0469\(1977\)034<1149:TIOPOT>2.0.CO;2](https://doi.org/10.1175/1520-0469(1977)034<1149:TIOPOT>2.0.CO;2), 1977.
- Wang, S., Wang, Q., Feingold, G.: Turbulence, Condensation, and Liquid Water Transport in Numerically Simulated Nonprecipitating Stratocumulus Clouds, *J. Atmos. Sci.*, 60, 262–278, [https://doi.org/10.1175/1520-0469\(2003\)060<0262:TCALWT>2.0.CO;2](https://doi.org/10.1175/1520-0469(2003)060<0262:TCALWT>2.0.CO;2), 2003.

- 605 Wang, Y., Ma, P., Jiang, J., Su, H., Rasch, P. J.: Toward reconciling the influence of atmospheric aerosols and greenhouse gases on light precipitation changes in Eastern China, *J. Geophys. Res. Atmos.*, 121, 5878–5887, <https://doi.org/10.1002/2016JD024845>, 2016.
- Wang, Y., Shen, X., Jiang, M.: Spatial-Temporal Variation Characteristics of Different Grades of Precipitation in Changbai Mountain from 1961 to 2018, *Clim. Environ. Res.*, 26, 227–238, 2021.
- 610 Wei, J., Huang, W., Li, Z., Xue, W., Peng, Y., Sun, L., Cribb, M.: Estimating 1-km-resolution PM2.5 concentrations across China using the space-time random forest approach, *Remote Sens. Environ.*, 231, 111221, <https://doi.org/10.1016/j.rse.2019.111221>, 2019.
- Wei, J., Li, Z., Lyapustin, A., Sun, L., Peng, Y., Xue, W., Su, T., Cribb, M.: Reconstructing 1-km-resolution high-quality PM2.5 data records from 2000 to 2018 in China: spatiotemporal variations and policy implications, *Remote Sens. Environ.*, 252, 112136, <https://doi.org/10.1016/j.rse.2020.112136>, 2021.
- 615 Wei, J., Li, Z.: ChinaHighPM2.5: High-resolution and High-quality Ground-level PM2.5 Dataset for China (2000–2023), National Tibetan Plateau Data Center, <https://doi.org/10.5281/zenodo.3539349>, 2024.
- Williams, A. S., Igel, A. L.: Cloud Top Radiative Cooling Rate Drives Non-Precipitating Stratiform Cloud Responses to Aerosol Concentration, *Geophys. Res. Lett.*, 48, e2021GL094740, <https://doi.org/10.1029/2021GL094740>, 2021.
- 620 Wu, J., Ling, C., Zhao, D., Zhao, B.: A counterexample of aerosol suppressing light rain in Southwest China during 1951–2011, *Atmos. Sci. Lett.*, 17, 1–7, <https://doi.org/10.1002/asl.682>, 2016.
- Wu, J., Zhang, L., Gao, Y., Zhao, D., Zha, J., Yang, Q.: Impacts of cloud cover on long-term changes in light rain in Eastern China, *Int. J. Climatol.*, 37, 4409–4416, <https://doi.org/10.1002/joc.5095>, 2017.
- 625 Wu, J., Zhang, L., Zhao, D., Tang, J.: Impacts of warming and water vapor content on the decrease in light rain days during the warm season over eastern China, *Clim. Dyn.*, 45, 1841–1857, <https://doi.org/10.1007/s00382-014-2438-4>, 2015.
- Wu, S.: Changing characteristics of precipitation for the contiguous United States, *Clim. Change*, 132, 677–692, <https://doi.org/10.1007/s10584-015-1453-8>, 2015.
- Xue, H., Feingold, G., Stevens, B.: Aerosol Effects on Clouds, Precipitation, and the Organization of Shallow Cumulus Convection, *J. Atmos. Sci.*, 65, 392–406, <https://doi.org/10.1175/2007JAS2428.1>, 2008.
- 630 Yang, X., Zhao, C., Zhou, L., Wang, Y., Liu, X.: Distinct impact of different types of aerosols on surface solar radiation in China, *J. Geophys. Res. Atmos.*, 121, 6459–6471, <https://doi.org/10.1002/2016JD024938>, 2016.
- Yang, Y., Zhang, C., Zhang, J., Wang, Y.: Changes in soil moisture and dryness and their response to climate change in the Guanzhong region, *Arid Zone Research*, 41, 261–271, <https://doi.org/10.13866/j.azr.2024.02.09>, 2024.
- 635 Yuan, Z., Zhang, Z., Yan, J., Liu, J., Hu, Z., Wang, Y., Cai, M.: Spatiotemporal characteristics of different grades of precipitation in Yellow River Basin from 1960 to 2020, *Arid Zone Research*, 41, 1259–1271, <https://doi.org/10.13866/j.azr.2024.08.01>, 2024.
- Zhang, S., Wu, J., Zhao, D., Xia, L.: Characteristics and reasons for light rain reduction in Southwest China in recent decades, *Prog. Phys. Geogr.*, 43, 643–665, <https://doi.org/10.1177/0309133319861828>, 2019.
- 640 Zhang, Y., Liu, C., You, Q., Chen, C., Xie, W., Ye, Z., Li, X., He, Q.: Decrease in light precipitation events in Huai River Eco-economic Corridor, a climate transitional zone in eastern China, *Atmos. Res.*, 226, 240–254, <https://doi.org/10.1016/j.atmosres.2019.04.027>, 2019.
- Zhang, Z., Wang, K.: Quantifying and adjusting the impact of urbanization on the observed surface wind speed over China from 1985 to 2017, *Fundamental Res.*, 1, 785–791, <https://doi.org/10.1016/j.fmre.2021.09.006>, 2021.
- 645 Zhao, C., Tie, X., Lin, Y.: A possible positive feedback of reduction of precipitation and increase in aerosols over eastern central China, *Geophys. Res. Lett.*, 33, <https://doi.org/10.1029/2006GL025959>, 2006.
- [Zhang, F., Wang, Y., Peng, J., Chen, L., Sun, Y., Duan, L., Ge, X., Li, Y., Zhao, J., Liu, C., Zhang, X., Zhang, G., Pan, Y., Wang, Y., Zhang, A. L., Ji, Y., Wang, G., Hu, M., Molina, M. J., Zhang, R.: An unexpected catalyst dominates formation and radiative forcing of regional haze, PNAS, 117\(8\), 3960–3966, <https://doi.org/10.1073/pnas.1919343117>, 2020.](https://doi.org/10.1073/pnas.1919343117)
- 650 Zhou, J., Zhi, R., Li, Y., Zhao, J., Xiang, B., Wu, Y., Feng, G.: Possible causes of the significant decrease in the number of summer days with light rain in the east of southwestern China, *Atmos. Res.*, 236, 104804, <https://doi.org/10.1016/j.atmosres.2019.104804>, 2020.

Zhang, R., Zhu, S., Zhang, Z., Zhang, H., Tian, C., Wang, S., Wang, P., Zhang, H.: Long-term variations of air pollutants and public exposure in China during 2000–2020, Sci. Total Environ. 2024, 930. <https://doi.org/10.1016/j.scitotenv.2024.172606>, 2024.

带格式的: 书目, 行距: 单倍行距